

# 1 **Neuronal patterning of the tubular collar cord is highly conserved** 2 **among enteropneusts but dissimilar to the chordate neural tube**

3 Sabrina Kaul-Strehlow<sup>1,2,3\*</sup>, Makoto Urata<sup>4</sup>, Daniela Praher<sup>3</sup> and Andreas Wanninger<sup>1</sup>

4 <sup>1</sup>Department for Integrative Zoology, University of Vienna, Althanstr. 14, 1090 Vienna,  
5 Austria

6 <sup>2</sup>Research Center for Marine Biology, Tohoku University, Asamushi, Aomori, Aomori 039-  
7 3501, Japan

8 <sup>3</sup>current address: Department for Molecular Evolution and Development, University of  
9 Vienna, Althanstr. 14, 1090 Vienna, Austria

10 <sup>4</sup>Noto Marine Laboratory, Division of Marine Environmental Studies, Institute of Nature and  
11 Environmental Technology, Kanazawa University, Ogi, Noto-cho, Ishikawa 927-0553, Japan.

12 \*Corresponding author. E-mail: [sabrina.kaul-strehlow@univie.ac.at](mailto:sabrina.kaul-strehlow@univie.ac.at)

## 13 **Abstract**

14 The dorsal neural tube of chordates and the ventral nerve cord of annelids exhibit a similar  
15 molecular mediolateral architecture. Accordingly, the presence of such a complex nervous  
16 system (CNS) has been proposed for their last common ancestor. Members of Enteropneusta,  
17 a group of non-chordate deuterostomes, possess a less complex CNS including a hollow  
18 neural tube, whereby homology to its chordate counterpart remains elusive. Since the  
19 majority of data on enteropneusts stem from *Saccoglossus kowalevskii*, a derived direct-  
20 developer, we investigated expression of key neuronal patterning genes in the indirect-  
21 developer *Balanoglossus misakiensis*.

22 The collar cord of *B. misakiensis* shows anterior *Six3/6* and posterior *Otx + engrailed*  
23 expression, in a region corresponding to the chordate brain. Neuronal *Nk2.1/Nk2.2* expression  
24 is absent. Interestingly, we found median *Dlx* and lateral *Pax6* expression domains, i.e., a  
25 condition that is reversed compared to chordates.

26 Comparative analyses reveal that CNS patterning is highly conserved among enteropneusts.  
27 *BmiDlx* and *BmiPax6* have no corresponding expression domains in the chordate brain, which  
28 may be indicative of independent acquisition of a tubular CNS in Enteropneusta and  
29 Chordata. Moreover, mediolateral architecture varies considerably among chordates and  
30 enteropneusts, questioning the presence of a vertebrate-like patterned nervous system in the  
31 last common deuterostome ancestor.

## 32 **Introduction**

33 The evolution of the bilaterian central nervous system (CNS) has been hotly debated for  
34 decades [1-6]. In this debate, enteropneust hemichordates (or acorn worms) have occupied a  
35 pivotal role. Enteropneusts are a group of hemichordate deuterostomes distantly related to  
36 vertebrates, which have retained a number of putative ancestral bilaterian features such as a  
37 biphasic life style and a bilateral symmetric body. Enteropneusts share some characteristics  
38 with chordates, such as gill slits and, at least partly, a tubular nervous system. For these  
39 reasons, enteropneusts are ideal candidates to unravel the evolution of the nervous system of  
40 Deuterostomia. The majority of enteropneust species belong to one of the three main families  
41 Harrimaniidae (e.g. *Saccoglossus kowalevskii*), Spengelidae (e.g. *Schizocardium*  
42 *californicum*) and Ptychoderidae (e.g. *Balanoglossus* spp., *Ptychodera flava*) [7]. Harrimaniid  
43 species develop directly into the juvenile worm, whereas spengelid and ptychoderid  
44 enteropneusts develop indirectly via a specific larval type, the tornaria. Morphologically, the  
45 nervous system of enteropneusts is described as a basiepidermal plexus with additional  
46 condensed regions. These comprise the proboscis stem and nerve ring, a dorsal nerve cord  
47 along the collar and trunk region, and a ventral nerve cord in the trunk connected to the dorsal  
48 nerve cord by a prebranchial nerve ring (Fig.1A') [8,9]. The dorsal nerve cord within the  
49 collar region, the 'collar cord', is a subepidermal tubular nerve cord that is often thought to be  
50 reminiscent of the chordate neural tube and, like the latter, forms by neurulation [10,11]. The  
51 collar cord is subdivided into a dorsal sheath of different neuronal cell types surrounding a  
52 central neural canal and a ventral neuropil [11,12]. Although these morphological features  
53 would support homology of the chordate neural tube and the collar cord of enteropneusts, it  
54 remains unclear to which part of the chordate neural tube the collar cord might correspond to.  
55 Moreover, the results from gene expression analyses are somewhat contradictory. The CNS of  
56 many bilaterians is patterned similarly from anterior to posterior by a number of specific  
57 transcription factors (see [3] for review). For instance, genes such as *Six3/6*, *Otx* and  
58 *engrailed* regionalize different parts of the brain in bilaterians, while *Hox* genes pattern the  
59 postcerebral region (spinal cord or ventral nerve cord, respectively). Anteroposterior  
60 patterning of these transcription factors has been studied in the enteropneust *S. kowalevskii*  
61 and is similar to that in chordates [3,13,14], yet the expression domains in enteropneusts are  
62 circumferential in the entire ectoderm and not restricted to the CNS-forming domains  
63 ("neuroectoderm") as in chordates [13,14]. Like in *S. kowalevskii*, a recent study described  
64 similar expression domains of those transcription factors in the spengelid *S. californicum* [15].  
65 To complicate things further, Miyamoto and Wada [16] showed that genes specifying the

66 chordate neural plate border (e.g., *SoxE*, and *Bmp2/4*) have conserved expression domains in  
67 the collar cord of the enteropneust *Balanoglossus simodensis* [16]. Concluding so far, no  
68 unequivocal homology statement can be made at present concerning the collar cord and the  
69 chordate neural tube.

70 Most of the molecular data available for enteropneusts have been obtained from *S.*  
71 *kowalevskii*, a harrimaniid with derived direct development. This data has been supplemented  
72 recently by a bodypatterning study of the spengelid *S. californicum* [15], yet comparable data  
73 from a ptychoderid species are still missing. However, a reliable ground pattern of neuronal  
74 patterning for Enteropneusta can only be reconstructed, if data from members of as many  
75 different enteropneust families are compared. Thus, in order to contribute new insights into  
76 the evolution of tubular nervous systems in Deuterostomia a comparable study on neuronal  
77 patterning of the collar cord in a ptychoderid enteropneust is of prime importance.

78 Here, we studied the expression domains of neuronal patterning genes in the indirectly  
79 developing ptychoderid *Balanoglossus misakiensis*, in order to provide the missing data. We  
80 focused on the expression patterns in the developing collar cord of anteroposterior (*Six3/6*,  
81 *Otx*, and *engrailed*) as well as so-called mediolateral patterning genes (*Pax6*, *Dlx*, *Nk2.1*,  
82 *Nk2.2*). The latter have been reported to form abutting domains of *Nk* and *Pax* genes in the  
83 annelid ventral nerve cord and in the vertebrate dorsal neural tube [2,17]. In each of these  
84 progenitor domains specific neuronal cell types are formed. For instance, serotonin-positive  
85 (+) neurons are exclusively restricted to the median *Nk2.1* domain in the brain and to the  
86 median *Nk2.2* in the trunk nerve cord [2]. *Pax6* forms two bilaterally symmetric, intermediate  
87 progenitor domains and *Dlx* two lateral domains. Given the complexity of the corresponding  
88 spatial organization of the annelid nerve cord and the vertebrate neural tube, a similarly  
89 patterned nervous system has been proposed in the Urbilaterian. Herein, we assess the  
90 presence of putative mediolateral patterning in the collar cord of *B. misakiensis*. This study  
91 comprises the first gene expression data for this particular species. Our data allow for a  
92 comparison with other enteropneusts and lead to a reliable ground pattern reconstruction for  
93 Enteropneusta. Eventually, this will help comparing the collar cord to the chordate neural tube  
94 and contribute to our understanding of nervous system evolution in Deuterostomia.

## 95 **Results**

### 96 **Neuronal differentiation of the adult nervous system**

97 The central nervous system of *B. misakiensis* including the collar cord become  
98 morphologically distinct in early settled juveniles, indicating that neurogenic patterning of the

99 collar cord starts in metamorphosing larvae [18]. In contrast, the larval nervous system (apical  
100 organ and neurite bundles of the ciliary bands) are independent of the adult nervous system  
101 and degrade during metamorphosis and settlement [7,16,19]. Therefore, we focused on the  
102 expression patterns in metamorphosing larvae and early juveniles.

103 In order to obtain an overview of the developing adult nervous system of *Balanoglossus*  
104 *misakiensis*, we first examined the expression of *Elav*, an RNA-binding protein that marks  
105 differentiating neurons [20-22]. *BmiElav* is expressed in the epidermis of the metamorphosing  
106 larva (Agassiz stage) of *B. misakiensis* as a stripe along the entire dorsal midline (except at the  
107 level of the telotroch) and extends circumferentially to the posterior base of the proboscis  
108 (Fig. 1A, B, D). In addition, *BmiElav* expression runs along the ventral midline of the trunk  
109 region with a gap in the region of the telotroch (Fig. 1A, C, D). *BmiElav* thus includes the  
110 region of the future dorsal and ventral nerve cords. Higher magnification of the perianal field  
111 reveals additional scattered *BmiElav*<sup>+</sup> cells laterally outside the nerve cords (Fig. 1E).

112 In juvenile *B. misakiensis*, *Elav*<sup>+</sup> cells are abundant in all condensed parts of the nervous  
113 system [18], including the proboscis plexus at the base of the proboscis region and the  
114 proboscis nerve ring (Fig. 1 A', B'). At the level of the collar region, *BmiElav*<sup>+</sup> cells locate to  
115 the subepidermal collar cord (Fig. 1D'). *BmiElav*<sup>+</sup> cells are also present in the prebranchial  
116 nerve ring, as well as in the dorsal and ventral nerve cords in the trunk region (Fig. 1B', C').  
117 The *BmiElav* signal is interrupted in the dorsal nerve cord at the former position of the  
118 telotroch.

### 119 **Gene expression of anteroposterior patterning genes**

120 We studied the expression of selected axial patterning genes in order to determine the region  
121 to which the enteropneust collar cord might correspond to in the vertebrate neural tube.

122 The transcription factor *BmiSix3/6* is strongly expressed throughout the entire ectoderm of the  
123 proboscis region and extends into the anterior rim of the collar ectoderm in metamorphosing  
124 larvae (Fig. 2A, B) and juvenile worms (Fig. 2C, D).

125 *BmiOtx* is expressed in the metamorphosing larva in the ventral area of the proboscis nerve  
126 ring (Fig. 2F) and in a distinct annular domain, encircling the anterior and middle collar  
127 region (Fig. 2E, F, Fig. S1B). The additional domain in the anterior pharyngeal region (Fig.  
128 2E arrowheads) is a non-neural endodermal domain that will not be further discussed. In the  
129 juvenile enteropneust *BmiOtx* is expressed in the ventral and ventrolateral area of the  
130 proboscis nerve ring (Fig. 2G, H). The expression forms a U-shaped domain at the position  
131 where the sensory 'pre-oral ciliary organ' develops (Fig. 2G inset). *BmiOtx* is also weakly

132 expressed throughout the ectoderm of the collar region (Fig. 2H). The signal within the  
133 proboscis coelom is due to probe trapping and interpreted as unspecific background (Fig. S1).  
134 *BmiEn* is expressed in a circumferential ring at the very posterior margin of the collar region  
135 in metamorphosing larvae (Fig. 2I, J and Fig. S1C). The signal is ectodermal and interrupted  
136 at the level of the dorsal midline. The juvenile enteropneust shows a similar expression  
137 pattern at the posterior margin of the collar region (Fig. 2K, L). The ring of *BmiEn* expression  
138 shows a gap on the dorsal side, as in the metamorphosing larva.  
139 In summary, the collar cord, that is part of the enteropneust collar region (mesosome), abuts  
140 anteriorly the expression domain of *BmiSix3/6*, lies within the *BmiOtx*-expression region, and  
141 is posteriorly delimited by a line of *BmiEn* expression.

### 142 **Gene expression of mediolateral patterning genes**

143 In metamorphosing larvae, *BmiPax6* is strongly expressed in the proboscis nerve ring at the  
144 base of the proboscis and in an additional circular pattern in the ectoderm of the posterior  
145 collar region (Fig. 3A, B). Between both circumferential domains, *BmiPax6* is also expressed  
146 in two parallel, longitudinal domains of the collar (Fig. 3A, dashed area). This area of the  
147 neural plate will later neurulate to form the subepidermal collar cord [11]. In juveniles,  
148 *BmiPax6* still shows a strong signal in the proboscis nerve ring. The circular domain in the  
149 posterior collar region becomes fainter in early juveniles (Fig. 3C inset) and is lost in older  
150 juveniles (Fig. 3C, D). No collar cord *BmiPax6* expression domains are present in juveniles.

151 Expression of *BmiDlx* is present in the proboscis nerve ring and along the dorsal nerve cord  
152 with an interruption at the level of the telotroch in the metamorphosing larva (Fig. 3E, F). In  
153 juveniles of *B. misakiensis* *Dlx* expression shows a faint signal in the ventral and ventrolateral  
154 portion of the proboscis nerve ring and in the dorsal nerve cord including the collar cord (Fig.  
155 3G, H). Our data show that *BmiDlx* is expressed in the collar cord and in the dorsal nerve cord  
156 and forms a single median domain.

157 *BmiNkx2.1* has four distinct expression domains in the metamorphosing larva (Fig. 3I, J). At  
158 this stage, the apical organ is degrading [18] and *BmiNkx2.1* is weakly expressed in this  
159 ectodermal region (Fig. 3I, J asterisk). *BmiNkx2.1* shows a strong expression domain in the  
160 ventral ectoderm at the base of the proboscis region (Fig. 3J unfilled arrowhead). Further  
161 strong domains are within the developing endodermal stomochord (Fig. 3I, double arrowhead)  
162 and medially in the posterior pharyngeal endoderm (Fig. 3I, J black arrowhead). A fifth,  
163 although weak signal, is present in the hindgut (Fig. 3J, white arrowhead).

164 The transcription factor *BmiNkx2.2* is strongly expressed in the lateral and dorsal portions of  
165 the anterior pharyngeal endoderm in the metamorphosing larva (Fig. 3K, inset, L). In the

166 juvenile worm the *BmiNkx2.2* domain has extended posteriorly and is present throughout the  
167 endoderm, but absent from the hindgut (Fig. 3M, N). Thus, there is no expression domain of  
168 *Nk2* genes in the collar cord or the trunk nerve cords in *B. misakiensis*.  
169 We additionally checked the distribution of serotonin-LIR neuronal components within the  
170 collar cord, because these neurons are restricted to the *Nkx2.1/2.2* domains in annelids and  
171 chordates. The serotonin-like immunoreactivity (LIR) nervous system of *B. misakiensis* has  
172 been described earlier [18], but the precise position of serotonin-LIR neurites within the collar  
173 cord has remained unknown. In the juvenile enteropneust serotonin-LIR neurons are present  
174 in the epidermis throughout all three body regions, with higher concentrations of somata in  
175 the proboscis and collar epidermis (Fig. 3O). Serotonin-LIR neurites form a basiepidermal  
176 nerve plexus in the proboscis and collar region. In the trunk region the serotonin-LIR neurites  
177 are condensed within the dorsal and ventral midline, in regions that constitute the nerve cords  
178 [18]. The neurulated collar cord passes through the mesocoel and is composed of a dorsal area  
179 of cells and a ventral neuropil (Fig. 3P, Q). The dorsal sheath of cells of the collar cord is  
180 devoid of serotonin-LIR somata (Fig. 3Q). Only two ventrolateral serotonin-LIR neurite  
181 bundles pass through the ventral neuropil. The lateral neurite bundles run adjacent to a pair of  
182 longitudinal muscle bundles that flank the collar cord (Fig. 3Q).

## 183 **Discussion**

184 We investigated the expression domains of several genes involved in axial as well as  
185 mediolateral patterning of the nervous system of the indirect developing enteropneust  
186 *Balanoglossus misakiensis*. By using the pan-neuronal marker *Elav* for differentiating neurons  
187 [20-22], we found that the major parts of the central nervous system already develop in  
188 metamorphosing larvae prior to settlement. Within the collar region, the neural plate of the  
189 future collar cord is present and still part of the epidermis. In juveniles of *B. misakiensis*, the  
190 neural plate has neurulated completely to form the subepidermal tubular collar cord as also  
191 reported in other enteropneust species [10,11,16].

## 192 **Gene expression patterning of the collar cord in Enteropneusta**

193 The transcription factors *Six3/6*, *Otx* and *engrailed* have been shown to play a conserved role  
194 in anteroposterior patterning and regionalization of the nervous system in chordates and in  
195 many other bilaterians [3]. It has been reported that *Six3/6* patterns the anteriormost region of  
196 the nervous system in numerous animals [3,23,24]. We found that in *B. misakiensis* the  
197 expression pattern of *Six3/6* is likewise at the anteriormost region of the animal, while *Otx*

198 and *engrailed* form circular epidermal domains around the collar and the posterior margin of  
199 the collar region, respectively (Fig. 4B'). These expression domains are spatially similar to  
200 what has been described in the spengelid *Schizocardium californicum* [15] as well as the  
201 harrimaniid enteropneust *Saccoglossus kowalevskii* (Fig. 4C', taken from [13,14])  
202 Accordingly, we suggest a conserved role of neuronal as well as body region patterning for  
203 *Six3/6*, *Otx* and *engrailed* in Enteropneusta that is independent from their mode of  
204 development (direct vs. indirect, Fig.4B-C''). It is moreover a plesiomorphic feature for  
205 Enteropneusta that has been inherited from a common bilaterian ancestor [3,13,23].

206 Next, we examined the expression pattern of *Dlx*, *Pax6* and *Nk2.1/2.2*. These transcription  
207 factors form mediolateral neurogenic domains in the neural tube of mouse, fruit fly as well as  
208 in the annelid *Platynereis dumerilii* [17,25]. Our analysis in *B. misakiensis* shows that *BmiDlx*  
209 is expressed in a narrow longitudinal stripe in the dorsal midline of the neural plate in *B.*  
210 *misakiensis* (Fig. 4B'). A similar pattern has been reported for *Dlx* in *S. kowalevskii* (Fig. 4C',  
211 after [14,26]), *S. californicum* [15] and *Balanoglossus simodensis* [16], suggesting a  
212 conserved role of this transcription factor in neurogenesis in Enteropneusta. We then verified  
213 the expression pattern of *BmiPax6* and found that it forms two lateral stripes along the neural  
214 plate of *B. misakiensis* (Fig. 4B'). We show that *BmiPax6* is only expressed for a short period  
215 in the neural plate during metamorphosis and is entirely absent in early juveniles (2 d ps) (Fig.  
216 3C, D). This is the only report of a distinct expression pattern of *Pax6* in the neural plate of an  
217 enteropneust species. In a comparable developmental stage of *S. kowalevskii* (1-gill-slit  
218 stage), *Pax6* is expressed in corresponding circular domains (Fig. 4C', after [13,14]), yet  
219 details from the neural plate are unknown. In *B. simodensis* and *S. californicum*, *Pax6*  
220 expression was not detected in the neural plate [15,16]. Thus, *Pax6* expression in the collar  
221 cord might be a species-specific acquisition of *B. misakiensis* and not part of the enteropneust  
222 ground pattern (Fig. 4A).

223 Expression pattern analysis of the median progenitor markers *Nk2.1* and *Nk2.2* revealed that  
224 there is no expression domain of either of the *BmiNk2* genes in the developing neural plate or,  
225 later, in the collar cord in *B. misakiensis*. Instead, the main domains of *Nk2.1* and *Nk2.2* are  
226 detected in the pharyngeal endoderm (Fig. 3I-N). In the direct developer *S. kowalevskii* a  
227 likewise endodermal expression of both genes has been reported previously [13,26] and in  
228 *Ptychodera flava* *Nk2.1* shows similar domains [27], suggesting a more general role in  
229 endoderm specification of these genes in enteropneusts [28]. Moreover, serotonergic neurons  
230 in vertebrates are usually restricted to the progenitor domains of *Nk2.1/2.2* [29]. Our data  
231 show that there is no median *Nk2.2* domain in the collar cord in *B. misakiensis*. Concordantly,

232 no serotonin-LIR somata are present in the collar cord of *B. misakiensis*. In fact, *Nk2.2* does  
233 not co-localise with serotonin-LIR neurons in *B. misakiensis*. It was shown that serotonin-LIR  
234 neurons are indeed present in enteropneusts, yet all of them comprise bipolar neurons  
235 throughout the epidermis of *B. misakiensis*, *S. kowalevskii* [18] as well as *P. flava* [12].  
236 Concluding so far, except for *Pax6*, the expression patterns of all the investigated genes in this  
237 study are highly congruent among the enteropneusts *S. kowalevskii*, *S. californicum*, *B.*  
238 *simodensis*, *P. flava* as well as *B. misakiensis*, which is why a similar function appears most  
239 likely. The data further reveals that neuronal patterning in the different families of  
240 Enteropneusta (Harrimaniidae, Spengelidae and Ptychoderidae) is not affected by different  
241 developmental modes. This conclusion is also supported by morphogenetic data of the  
242 developing nervous system in enteropneusts [18]. On that basis, we propose that a similar  
243 collar cord patterning was present in the last common ancestor of Enteropneusta (Fig. 4A).  
244 These results further corroborate the suitability of indirect as well as direct developing  
245 enteropneusts for serving as model organisms to conduct ‘evodevo’ studies in hemichordates.

#### 246 **Comparative aspects of neural tube patterning among deuterostomes**

247 Morphological similarities between the tubular collar cord and the chordate neural tube have  
248 not gone unnoticed and have been acknowledged from early on [30]. Therefore, we compare  
249 here the gene expression patterns of the studied transcription factors among different  
250 deuterostomes and discuss evolutionary implications.

251 Chordata comprises three major taxa, Cephalochordata, Tunicata and Vertebrata, of which the  
252 latter two form the monophyletic Olfactores [31,32]. All three groups share corresponding  
253 expression domains of the transcription factors *Six3/6*, *Otx* and *Engrailed (En)* (Fig. 4D-F),  
254 which are restricted to the anterior portion of the neural plate, i.e., the future brain region  
255 [3,33]. Thereby, coexpression of *Otx* and *En* mark the midbrain-hindbrain boundary (MHB)  
256 in vertebrates and the posterior margin of the sensory vesicle (brain) in the ascidian *Ciona*  
257 *intestinalis*. In contrast, the coexpressing domain of *Otx* and *En* in amphioxus is located in  
258 the midlevel of the brain region, whereas a second expression domain of *Six3/6* is present at  
259 the posterior end of the cerebral vesicle (Fig. 4D) [3,34]. Moreover, all three groups show a  
260 median/ventral *Nk2.1* domain and expression domains of *Pax6* and *Dlx* in the brain region  
261 [13,17,29,35-39]. Thus, the chordate ancestor likely had a similar brain patterned by these  
262 transcription factors [3].

263 Mediolateral patterning of the postcerebral part of the neural tube by *Pax6*, *Dlx* and *Nk2.1/2.2*  
264 differs considerably between chordates and needs further attention. The specific arrangement  
265 of lateral *Dlx*, mediolateral *Pax6* and median *Nk2* domains has been reported from the

266 vertebrate spinal cord and hindbrain levels (posterior to MHB) as well as the annelid and  
267 insect ventral nerve cord (postcerebral) [2,3]. The median column of *Nk2.2* is an exception as  
268 its domain projects anteriorly throughout the midbrain region and is replaced by *Nk2.1* in the  
269 vertebrate forebrain (Fig. 4F). However, ascidians share only a mediolateral *Pax6* domain  
270 with vertebrates, while *Dlx* and *Nk2.2* expression is absent from the postcerebral neural tube  
271 (Fig. 4E) [3,39,40]. Ascidians belong to Tunicata, a taxon of rapidly evolving animals with  
272 reduced genome size that have lost about 25 genes involved in developmental patterning  
273 including *Gbx*, *Wnt1* and *Nk2.2* [33,41,42]. Thus, the aberrant and lacking expression  
274 domains compared to vertebrates might be explained by secondary gene losses in Tunicata.  
275 Compared with this, amphioxus does not appear to be rapidly evolving. In fact,  
276 cephalochordates have retained all of the putative ancestral bilaterian homeobox genes  
277 [33,42] and the genome of amphioxus is supposed to represent the most ancestral one among  
278 chordates, in parallel to a less derived morphology [42]. However, *Pax6* and *Dlx* expression  
279 are absent from the nerve cord in amphioxus, instead the median *Nk2.1* domain extends  
280 throughout the posterior neural plate (Fig. 4D) [38]. It should be mentioned here, that a  
281 median *Nk2.1/2.2* domain, a mediolateral *Pax6* as well as a lateral *Dlx* expression domain is  
282 very well present in amphioxus, yet these expression domains are located in the posterior  
283 region of the cerebral vesicle (Fig. 4D) and not in the postcerebral CNS as in vertebrates (Fig.  
284 4D, F) and the protostomes *Platynereis dumerilii* and *Drosophila melanogaster* [2,17]. Taken  
285 together, mediolateral expression domains of *Pax6*, *Dlx* and *Nk2* genes differ considerably  
286 among chordates, making it difficult to postulate a ground pattern for the last common  
287 chordate ancestor.

288 Since vertebrates and annelids (which exhibit a similar mediolateral patterning) are only  
289 distantly related taxa and comparable data from most intermediate groups are missing (see  
290 also [5]), an outgroup comparisons with Enteropneusta is most reasonable; not least, because  
291 this taxon is part of the Ambulacraria, the sister group of Chordata [32]. Comparison of the  
292 expression domains of *Six3/6*, *Otx* and *En* leads to the suggestion that the collar cord in  
293 enteropneusts might correspond to a region of the chordate brain rather than to the  
294 postcerebral neural tube (Fig. 4A, D-F). This is also supported by comparative Hox gene  
295 expression analysis in *S. kowalevskii* [3,13]. In Enteropneusta the neural plate is patterned  
296 medially by *Dlx* ([13,14,16] this study) (Fig. 4A), whereas *Dlx* expression is restricted to the  
297 very lateral area of the brain in amphioxus and ascidians (Fig. 4D, E) and the spinal cord in  
298 vertebrates (Fig. 4F). Accordingly, there is no corresponding mediolateral patterning present  
299 in the enteropneust nervous system, and compared to chordates the expression domains of *Dlx*

300 and *Pax6* are flipped in *B. misakiensis* (Fig. 4B', D-F). These incongruent expression patterns  
301 might be explained by the fact that dorsoventral signaling of *Bmp* and *chordin*, which is  
302 responsible for the placement of the mediolateral patterning domains, is inverted in  
303 enteropneusts and chordates [26]. It was shown in *S. kowalevskii* that the tubular collar cord  
304 develops from the *Bmp*-expressing side, whereas the dorsal neural tube of chordates and the  
305 ventral nerve cord of protostomes form at the *Chordin*-expressing side [26,43]. Concordantly,  
306 markers of midline cells in the chordate neural tube such as *Sim* and *Netrin* are expressed in  
307 the ventral ectoderm in enteropneusts while lateral markers of the chordate neural tube such  
308 as *Dlx* are expressed in the dorsal ectoderm ([26], this study). Thus, according to the  
309 dorsoventral (D-V) inversion hypothesis [44,45], the collar cord might in fact be positioned  
310 on the “wrong side”, that is, corresponding to the ventral side of chordates.

## 311 **Conclusion**

312 A complex mediolateral patterning of the postcerebral nervous system by *Pax6*, *Dlx* and  
313 *Nk2.1/Nk2.2*, among others, has been reported from vertebrates and the protostomes  
314 *Platynereis dumerilii* and *Drosophila melanogaster* [2,3,17]. However, comparison of their  
315 expression domains among different deuterostome taxa does not suggest that a likewise  
316 patterned postcerebral nervous system was present in the last deuterostomian ancestor (Fig.  
317 4). Moreover, the tubular collar cord of Enteropneusta shows no expression domains of *Dlx* or  
318 *Pax6* that clearly correspond to the chordate brain. The “flipped” domains of *Dlx* and *Pax6* in  
319 enteropneusts are likely the result of an inverted *BMP/Chordin* expression compared to  
320 chordates [26], and suggest that the collar cord represents an independent acquisition of  
321 Enteropneusta, thereby contrasting the results from ultrastructural and classical investigations  
322 [10,11]. Accordingly, the question of homology versus independent evolution of the  
323 enteropneust collar cord and the chordate neural tube might primarily depend on the  
324 (subjective) decision whether one favors the morphogenetic over the molecular (gene  
325 expression) evidence or vice versa. While this may sound frustrating at first, the incongruence  
326 in the dataset currently available should instead motivate today’s developmental biologists to  
327 further engage in research into this area in order to finally settle one of the key issues in  
328 animal evolution: the origin of bilaterian centralized nervous systems.

## 329 **Materials & Methods**

### 330 ***Balanoglossus misakiensis* (Kuwano, 1902)**

331 Adult *B. misakiensis* were collected at a depth of 1 to 2 m at Sunset beach, Aomori-Bay,  
332 Asamushi, Aomori, Japan, in June 2012 and June 2014. Specimens were transported to the  
333 Research Center for Marine Biology Tohoku University in Asamushi and were kept in aquaria  
334 with running filtered seawater at ambient water temperature (24 - 26°C) as previously  
335 described [18,46]. Spawning, in vitro fertilization, and fixations were performed as described  
336 earlier [18].

### 337 **Immunolabelling and confocal laser scanning microscopy**

338 Juveniles of *B. misakiensis* (2-gill-slit juvenile = 3 days post settlement) were fixed with 4%  
339 paraformaldehyde (PFA) in phosphate buffer (PBS). Specimens were processed using  
340 standard protocols as previously described [18].

### 341 **RNA extraction, transcriptome analysis and gene cloning**

342 More than 1,000 larvae from developmental stages of *B. misakiensis* ranging from early  
343 hatched tornaria to three day old juvenile worms were fixed in RNAlater (Sigma). Total RNA  
344 was extracted from a mix of developmental stages using RNeasy Mini Kit from Qiagen.  
345 Extracted RNA was sent to Eurofins (Germany) for Illumina HiSeq 2000 sequencing using  
346 paired-end read module resulting in reads of 100bp length. Obtained reads were assembled to  
347 contigs using Trinity software under standard parameters and the transcriptome was analysed  
348 for sequences of interest with BLAST search in Geneious 6.1 (Biomatters, New Zealand).  
349 Primers were generated to obtain fragments of *Elav*, *Six3/6*, *Pax6*, *Dlx*, *Otx*, *Engrailed*, *Nk2.1*  
350 and *Nk2.2* (for primer sequences and accession numbers see supplemental material) in order  
351 to sub-clone into pGemT Easy vector (Promega).

### 352 **Phylogenetic analysis**

353 Full protein sequences were aligned using MUSCLE and Regions with low-quality  
354 alignments for the Elav phylogenetic analysis were trimmed by TrimAl 1.2 rev 59 [47].  
355 ProtTest 2.4 [48] analysis retrieved LG (+G+F) and JTT (+I+G+F) for the Elav (Fig. S2) and  
356 the homeobox protein (Fig. S3) analyses respectively as best-fitting models for the  
357 phylogenetic reconstruction. The maximum likelihood tree was then generated with PhyML  
358 3.0 ([49], BIONJ input tree, optimised tree topology, 4 substitution rate categories, best of  
359 NNI and SPR, 100 non-parametric bootstrap replicates).

## 360 **Probe synthesis and *in situ* hybridization**

361 Chromogenic *in situ* hybridizations were performed on whole-mounts following the protocol  
362 from Röttinger and Martindale [50] with minor adjustments for *B. misakiensis*.  
363 Metamorphosing larvae (Agassiz stage) and juveniles (2-gill-slit stage) were treated with 10  
364 ng/μl Proteinase K (Roth) for 4 min at room temperature. Colour development was stopped  
365 by three washes in PTw (phosphate buffered saline + 0.1% Tween20) and postfixed with 4%  
366 PFA for 1 hour. Animals were transferred into 100% EtOH over night for clearing and  
367 mounted in 80% glycerol.

## 368 **Controls**

369 Controls with sense probes were conducted in order to identify unspecific binding and probe  
370 trapping during *in situ* hybridization. The protocol within the proboscis region turned out to  
371 be a perfect trap for any probe (Fig. S1A). Perforation of the proboscis using a thin tungsten  
372 needle helped to solve this problem (Fig.S1D, E). However, probe trapping could not always  
373 be eliminated, which is why a blue protocol persists in the *in situ* hybridizations of *Dlx*  
374 (Fig.3E-H) and in *Otx* and *engrailed* in juveniles (Fig.2G, H, K, L).

## 375 **References**

- 376 1. Holland ND (2003) Early central nervous system evolution: An era of skin brains? Nat  
377 Rev Neurosci 4:1–11.
- 378 2. Arendt D, Denes AS, Jekely G, Tessmar-Raible K (2008) The evolution of nervous  
379 system centralization. Phil Trans R Soc B 363: 1523–1528.
- 380 3. Holland LZ, Carvalho JE, Escrava H, Laudet V, Schubert M, Shimeld S, Yu J-K (2013)  
381 Evolution of bilaterian central nervous systems: a single origin? EvoDevo 4:27.
- 382 4. Arendt D, Tosches MA, Marlow H (2015) From nerve net to nerve ring, nerve cord and  
383 brain – evolution of the nervous system. Nature Rev Neurosci 17: 61-72.
- 384 5. Hejnol A, Lowe CJ (2015) Embracing the comparative approach: how robust phylogenies  
385 and broader developmental sampling impacts the understanding of nervous system  
386 evolution. Phil. Trans. R. Soc. B 370: 20150045.
- 387 6. Lowe CJ, Clarke DN, Medeiros DM, Rokhsar DS, Gerhart J (2015) The deuterostome  
388 context of chordate origins. Nature 520: 456-465.
- 389 7. Kaul-Strehlow S, Röttinger E (2015) *Hemichordata* in: Evolutionary developmental  
390 biology of invertebrates Vol. 6 (ed. Andreas Wanninger). Springer Verlag, Berlin.

- 391 8. Bullock TH (1946) The anatomical organization of the nervous system of Enteropneusta.  
392 Q J Microsc Sci 86: 55-112.
- 393 9. Knight-Jones EW (1952) On the nervous system of *Saccoglossus cambrensis*  
394 (Enteropneusta). Philos Trans R Soc Lond B 236: 315–354.
- 395 10. Morgan TH (1894) The development of Balanoglossus. J Morphol 9: 1–86.
- 396 11. Kaul S, Stach T (2010) Ontogeny of the collar cord: Neurulation in the hemichordate  
397 *Saccoglossus kowalevskii*. J Morph 271: 1240–1259.
- 398 12. Nomaksteinsky M, Roettinger E, Dufour HD, Chettouh Z, Lowe CJ, Martindale MQ,  
399 Brunet J-F (2009) Centralization of the Deuterostome Nervous System Predates  
400 Chordates. Curr Biol 19:1264–1269.
- 401 13. Lowe CJ, Wu M, Salic A, Evans L, Lander E, Stange-Thomann N, Gruber CE, Gerhart J,  
402 Kirschner M. (2003) Anteroposterior patterning in hemichordates and the origin of the  
403 chordate nervous system. Cell 113: 853–865.
- 404 14. Pani A, Mullarkey EE, Aronowicz J, Assimacopoulos S, Grove EA, Lowe CJ (2012)  
405 Ancient deuterostome origins of vertebrate brain signalling centres. Nature 438: 289–295.
- 406 15. Gonzalez P, Uhlinger KR, Lowe CJ (2017) The Adult Body Plan of Indirect Developing  
407 Hemichordates Develops by Adding a Hox-Patterned Trunk to an Anterior Larval  
408 Territory. Curr Biol 27: 87-95.
- 409 16. Miyamoto N, Wada H (2013) Hemichordate neurulation and the origin of the neural tube.  
410 Nat Commun 4:2713.
- 411 17. Denes AS, Jékely G, Steinmetz PRH, Raible F, Snyman H, Prud'homme B, Ferrier DEK,  
412 Balavoine G, Arendt D (2007) Molecular architecture of annelid nerve cord supports  
413 common origin of nervous system centralization in Bilateria. Cell, 129:277–288.
- 414 18. Kaul-Strehlow S, Urata M, Minokawa T, Stach T, Wanninger A (2015) Neurogenesis in  
415 directly and indirectly developing enteropneusts: of nets and cords. Org. Divers. Evol. 15,  
416 405–422. (doi:10.1007/s13127-015-0201-2)
- 417 19. Nielsen C, Hay-Schmidt A (2007) Development of the enteropneust *Ptychodera flava*:  
418 ciliary bands and nervous system. J Morphol 268:551–570.
- 419 20. Soller, M., and White, K. (2004). Elav. Curr. Biol. 14, R53.
- 420 21. Berger, C., Renner, S., Lüer, K., Technau, G.M., 2007. The commonly used marker  
421 ELAV is transiently expressed in neuroblasts and glial cells in the Drosophila embryonic  
422 CNS. Dev. Dyn. 236, 3562–3568.
- 423 22. Pascale, A., Amadio, M., Quattrone, A. (2008). Defining a neuron: neuronal ELAV  
424 proteins. Cell Mol Life Sci 65: 128-140.

- 425 23. Steinmetz, P. R. et al. Six3 demarcates the anteriormost developing brain region in  
426 bilaterian animals. *Evodevo* 1, 14 (2010).
- 427 24. Marlow H et al.: Larval body patterning and apical organs are conserved in animal  
428 evolution. *BMC Biology* 2014 12:7.
- 429 25. Holland LZ (2015) The origin and evolution of chordate nervous systems. *Phil. Trans. R.*  
430 *Soc. B* 370: 20150048. <http://dx.doi.org/10.1098/rstb.2015.0048>
- 431 26. Lowe CJ, Terasaki M, Wu M, Freeman RM, Runft L, Kwan K, Haigo S, Aronowicz J,  
432 Lander E, Gruber C, Smith M, Kirschner M, Gerhart J (2006) Dorsoventral patterning in  
433 hemichordates: insights into early chordate evolution. *PLoS Biol* 4: e291.
- 434 27. Takacs, CN., Moy, VN, Peterson, KJ (2002) Testing putative hemichordate homologues  
435 of the chordate dorsal nervous system and endostyle: expression of *NK2.1* (TTF-1) in the  
436 acorn worm *Ptychodera flava* (Hemichordata, Ptychoderidae). *Evol & Dev* 4: 405-417.
- 437 28. Okkema, P.G., Ha, E., Haun, C., Chen, W., and Fire, A. (1997) The *Caenorhabditis*  
438 *elegans* NK-2 homeobox gene *ceh-22* activates pharyngeal muscle gene expression in  
439 combination with *pha-1* and is required for normal pharyngeal development.  
440 *Development* 124, 3965–3973.
- 441 29. Shimamura, K., Hartigan, D. J., Martinez, S., Puelles, L. & Rubenstein, J. L. (1995)  
442 Longitudinal organization of the anterior neural plate and neural tube. *Development* 121:  
443 3923–3933.
- 444 30. Bateson W (1884) The early stages of the development of *Balanoglossus* (sp. incert.). *Q J*  
445 *Microsc Sci*, NS 24: 208-236, pls 18-21.
- 446 31. Delsuc F, Brinkmann H, Chourrout D, Philippe, H (2006) Tunicates and not  
447 cephalochordates are the closest living relatives of vertebrates. *Nature* 439: 965-968.
- 448 32. Cannon JT, Vellutini BC, Ill JS, Ronquist F, Jondelius U, Jejnol A (2016)  
449 Xenacoelomorpha is the sister group to Nephrozoa. *Nature* 530: 89-93.
- 450 33. Castro LFC, Rasmussen SLK, Holland PWH, Holland ND, Holland LZ (2006) A *Gbx*  
451 homeobox gene in amphioxus: Insights into ancestry of the ANTP class evolution of the  
452 midbrain/hindbrain boundary. *Dev Biol* 295: 40-51.
- 453 34. Kozmik Z, Holland ND, Kreslova J, Oliveri D, Schubert M, Jonasova K, Holland LZ,  
454 Pestarino M, Benes V, Candiani S (2007) *Pax-Six-Eya-Dach* network during amphioxus  
455 development: Conservation *in vitro* but context specificity *in vivo*. *Dev Biol* 306: 143-  
456 159.
- 457 35. Holland ND, Panganiban G, Henyey EL, Holland LZ (1996) Sequence and  
458 developmental expression of *AmphiDll*, an amphioxus *Distal-less* gene transcribed in the

- 459 ectoderm, epidermis and nervous system: insights into evolution of craniate forebrain and  
460 neural crest. *Development* 122: 2911-2920.
- 461 36. Mastick, G. S., Davis, N. M., Andrew, G. L. & Easter Jr, S. S. (1997) Pax-6 functions in  
462 boundary formation and axon guidance in the embryonic mouse forebrain. *Development*  
463 124: 1985–1997.
- 464 37. Gclardon S, Holland LZ, Gehring WJ, Holland ND (1998) Isolation and developmental  
465 expression of the amphioxus *Pax-6* gene (*AmphiPax-6*): insights into eye and  
466 photoreceptor evolution. *Development* 125: 2701-2710.
- 467 38. Venkatesh TV, Holland ND, Holland LZ, Su M-T, Bodmer R (1999) Sequence and  
468 developmental expression of amphioxus *AmphiNk2-1*: insights into the evolutionary  
469 origin of the vertebrate thyroid gland and forebrain. *Dev Genes Evol* 209: 254-259.
- 470 39. Irvine SQ, Cangiano MC, Millette BJ, Gutter ES (2007) Non-overlapping Expression  
471 Patterns of the Clustered *Dll-A/B* Genes in the Ascidian *Ciona intestinalis*. *J Exp Zool B*  
472 308: 428-441.
- 473 40. Edvardsen RB, Seo H-C, Jensen MF, Mialon A, Mikhaleva J, Bjordal M, Cartry J,  
474 Reinhardt R, Weissenbach J, Wincker P, Chourrout D (2005) Remodelling of the  
475 homeobox gene complement in the tunicate *Oikopleura dioica*. *Curr Biol* 15: R12-R13.
- 476 41. Holland LZ (2009) Chordate roots of the vertebrate nervous system: expanding the  
477 molecular toolkit. *Nat Rev* 10: 736-746.
- 478 42. Holland ND (2010) From genomes to morphology: a view from amphioxus. *Acta Zool*  
479 91: 81-86.
- 480 43. De Robertis EM (2008) Evo-Devo: Variations on Ancestral Themes. *Cell* 132: 185-195.
- 481 44. Geoffrey St-Hilaire E (1822) Considérations générales sur la vertèbre. *Mémoires, Mus*  
482 *d'His Nat* 9:89-119.
- 483 45. Arendt, D., and Nübler-Jung, K. (1999) Comparison of early nerve cord development in  
484 insects and vertebrates. *Development* 126, 2309–2325.
- 485 46. Urata M, Yamaguchi M (2004) The Development of the Enteropneust Hemichordate  
486 *Balanoglossus misakiensis* KUWANO. *Zoological Science* 21: 533–540.
- 487 47. Capella-Gutiérrez S, Silla-Martínez JM, Gabaldón T (2009) trimAl: a tool for automated  
488 alignment trimming in large-scale phylogenetic analyses. *Phylogenetics* 25: 1972-1973.
- 489 48. Abascal F, Zardoya R, Posada D (2005) ProtTest: selection of best-fit models of protein  
490 evolution. *Phylogenetics* 21: 2104-2105.

- 491 49. Guindon S, Dufayard J-F, Lefort V, Anisimova M, Hordijk W, Gascuel O (2010) New  
492 Algorithms and Methods to Estimate Maximum-Likelihood Phylogenies: Assessing the  
493 Performance of PhyML 3.0. *Syst Biol* 59: 307-321.
- 494 50. Röttinger, E. and Martindale, M. Q. (2011). Ventralization of an indirect developing  
495 hemichordate by NiCl suggests a conserved mechanism of dorso-ventral (D/V) patterning  
496 in Ambulacraria (hemichordates and echinoderms). *Dev. Biol.* 354: 173-190.
- 497 51. Holland LZ, Venkatesh TV, Gorlin A, Bodmer R, Holland ND (1998) Characterization  
498 and developmental expression of *AmphiNk2-2*, an NK2 class homeobox gene from  
499 amphioxus (Phylum Chordata; Subphylum Cephalochordata). *Dev Genes Evol* 208: 100-  
500 105.
- 501 52. Moret F, Christiaen L, Deyts C, Blin M, Joly J-S, Vernier P (2005) The dopamine-  
502 synthesizing cells in the swimming larva of the tunicate *Ciona intestinalis* are located  
503 only in the hypothalamus-related domain of the sensory vesicle. *Europ J Neurosci* 21:  
504 3043-3055.
- 505 53. Hudson C, Lemaire P (2001) Induction of anterior neural fates in the ascidian *Ciona*  
506 *intestinalis*. *Mech Dev* 100: 189-203.
- 507 54. Mazet F, Hutt JA, Millard J, Shimeld SM (2003) Pax gene expression in the developing  
508 central nervous system of *Ciona intestinalis*. *Gene Exp Patt* 3: 743-745.

## 509 **Acknowledgements**

510 We thank Takuya Minokawa from the Research Center for Marine Biology Tohoku  
511 University in Asamushi, Japan for, providing laboratory space and equipment. This study was  
512 funded by a Lise-Meitner grant from the Austrian Science Fond (FWF) to SK-S (M 1485-  
513 B19). The collection trip of SK-S to Japan was financially supported by a stipend from the  
514 Research Center for Marine Biology, Tohoku University, Japan. Tim Wollesen (University  
515 Vienna) is thanked for his help in basic molecular biological methods. SK-S thanks Thomas  
516 Eder and Thomas Rattei (both University of Vienna) for their kind assistance with Illumina  
517 transcriptome assembly. SK-S kindly acknowledges the valuable support of Eric Röttinger  
518 (University of Nice) and Grigory Genikhovich (University of Vienna) that allowed the  
519 establishment of a reliable in situ protocol for *B. misakiensis*. Patrick Steinmetz (Sars Center,  
520 Bergen) is thanked for critical comments and suggestions on earlier versions of this  
521 manuscript.

## 522 **Author Contributions**

523 SK-S and AW designed the study. MU and SK-S collected and cultured material. SK-S  
524 conducted IHC and cLSM analyses. SK-S extracted RNA, assembled the transcriptome,  
525 cloned all gene sequences, and performed in situ hybridizations. DP aligned sequences,  
526 conducted phylogenetic analyses and built orthology trees of the genes. SK-S wrote the  
527 manuscript with input from AW. All authors read, provided input, and approved the final  
528 version of the manuscript.

## 529 **Accession codes**

530 All gene sequences will be deposited at GenBank upon acceptance of this manuscript.

## 531 **Competing interests**

532 The authors declare that they have no competing financial interests.

## 533 **Figure Legends**

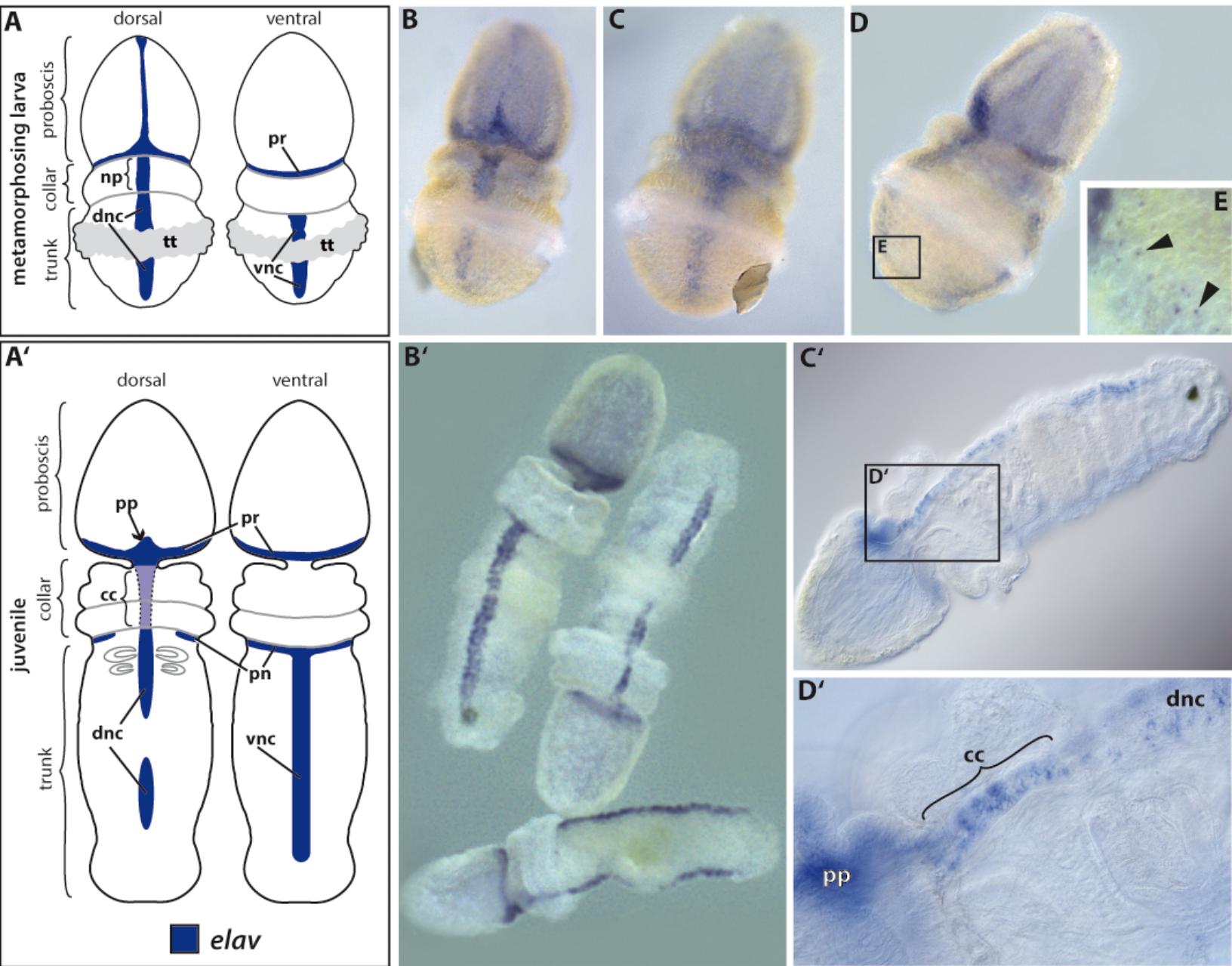
534 **Fig. 1 Establishment of the adult nervous system. Gene expression of *BmiElav* in the**  
535 **metamorphosing larva and juvenile of *B. misakiensis*. A-E** Metamorphosing larva. **A'-D'**  
536 Juvenile. **A** Schematic illustration of *BmiElav* expression. *BmiElav* is expressed in the  
537 proboscis nerve ring, the developing dorsal nerve cord including the neural plate in the collar  
538 (**B, D**) and in the ventral nerve cord (**C, D**). Note that the expression is interrupted at the level  
539 of the telotroch. **E** Detail of the lateral trunk showing scattered neurons (arrowheads). **A'**  
540 Schematic illustration of *BmiElav* expression in juveniles. Note that the collar cord is  
541 neurulated. **B'** Surface view from ventral, dorsal and lateral right (from top to bottom)  
542 showing strong expression in the proboscis nerve ring, proboscis plexus, and in the dorsal as  
543 well as ventral nerve cord. *BmiElav* expression is discontinuous in the middle of the dorsal  
544 nerve cord in the trunk region. **C'** Micrograph of cleared juvenile. **D'** Detail showing *Elav*+  
545 cells in the subepidermal collar cord. cc = collar cord, dnc = dorsal nerve cord, np = neural  
546 plate, pn = peribranchial nerve ring, pr = proboscis nerve ring, pp = proboscis plexus, tt =  
547 telotroch, vnc = ventral nerve cord. B dorsal view. C ventral view. D view from lateral right.

548 **Fig. 2 Anteroposterior patterning genes allocate the collar cord of *B. misakiensis* to the**  
549 **chordate brain region.** Anterior is to the top left. **A-D** *BmiSix3/6* is expressed throughout the

550 ectoderm of the proboscis region and the anterior collar. **E-H** *BmiOtx* is expressed  
551 circumferentially in the posterior proboscis ectoderm and in the ectoderm of the collar region.  
552 **E** Dorsal view showing an additional domain in the pharyngeal endoderm (arrowheads). **G**  
553 *BmiOtx* is strongly expressed in the preoral ciliary organ (arrowhead). Section plane of inset  
554 indicated by dashed line. Inset shows *Otx* expression in the ciliary organ of the proboscis in a  
555 cross section of the posterior proboscis. **I-L** *BmiEn* is expressed in a narrow ring in the  
556 ectoderm of the posterior end of the collar region with an interruption on the dorsal side. co =  
557 collar. A, C, E, G, I, K: dorsal views. B, D, F, H, J, L: ventral views.

558 **Fig. 3 Expression domains of mediolateral patterning genes and serotonin-LIR in *B.***  
559 ***misakiensis*.** **A, B** *BmiPax6* is expressed in the proboscis nerve ring and in a second  
560 circumferential domain in the collar ectoderm. Additionally, *BmiPax6* forms paired  
561 longitudinal domains in the neural plate (dashed area) of the developing larva. In juveniles,  
562 the expression in the collar ectoderm fades (inset) and only the proboscis nerve ring shows  
563 strong signal of *BmiPax6* (**C, D**). **E-H** *BmiDlx* is expressed as a median stripe in the collar  
564 and dorsal cord (arrowheads) with an interruption at the level of the telotroch (**E**). The strong  
565 staining in the protoceol is unspecific (see also Fig. S1). **I, J** Expression of *BmiNk2.1* in the  
566 metamorphosing larva. *BmiNk2.1* is strongly expressed in the stomochord (double  
567 arrowhead), in the ventrolateral ectoderm at the base of the proboscis (open arrowhead), in the  
568 posterior pharynx (black arrowhead), and weakly in the hindgut (white arrowhead). The  
569 degrading apical organ shows a faint signal (asterisk). **K-N** Expression of *BmiNk2.2*. **K**  
570 Surface view from ventral showing bilateral domains in the mid-pharynx region. **L** Lateral  
571 view from left. Inset shows a cross section of the collar region with the ventrolateral domain  
572 of *BmiNk2.2* in the pharyngeal endoderm. In juveniles the expression domain of *Nk2.2* is  
573 extended throughout the entire endoderm (**M, N**). Note that there is no ectodermal or neuronal  
574 expression domain of *BmiNk2.2*. **O-Q** Serotonin-LIR in the juvenile. **O** Overview. **P** Detail of  
575 the collar region as indicated in G. Partial Z-projection focussing on the collar cord (dashed  
576 area). **Q** Virtual cross section of the collar cord as indicated in H. Note that 5-HT+ somata are  
577 absent from the collar cord (dashed area). Only two ventrolateral 5-HT+ neurite bundles pass  
578 the neuropil. cc = collar cord, co = collar, ep = epidermis, g s= sill slit, lm = longitudinal  
579 muscles, nc = neural canal, pr = proboscis, sn = serotonin-LIR neuron, snb = serotonin-LIR  
580 neurite bundle, tr = trunk. A, C, E, G, I, K, M: dorsal views, B, J, L, N: lateral views left, D,  
581 F, H: ventral views.

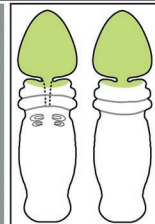
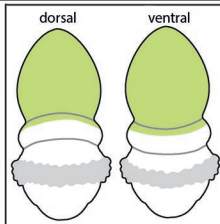
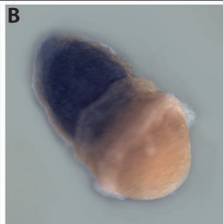
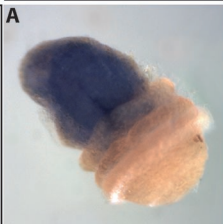
582 **Fig. 4 Comparison of axial patterning genes in the neural plate of diverse**  
583 **deuterostomian taxa with focus on different developing modes in enteropneusts.**  
584 Neuronal patterning in enteropneusts is highly conserved and independent of the mode of  
585 development. The ancestral condition of mediolateral patterning for Deuterostomia remains  
586 elusive. See text for discussion. **A** Expression domains of the hypothetical enteropneust  
587 ancestor. **B-B''** Selected developmental stages of *B. misakiensis*. **B** Metschnikoff larval stage.  
588 **B'** Metamorphosing Agassiz larval stage (this study). **B''** Juvenile worm. **C-C''** Selected  
589 developmental stages of *S. kowalevskii*. **C** Torpedo embryo stage. **C'** 1-gill slit hatchling  
590 (after data from [13,14]). **C''** Juvenile worm. **D** Expression domains in the neural plate of  
591 *Branchiostoma floridae* (after data from [33-35,37,38,51]). **E** Expression domains in the  
592 neural plate of the ascidian *Ciona intestinalis* (after data from [33,39,52-54]). **F** Expression  
593 domains in the neural plate of the vertebrate *Mus musculus*. Scheme modified after [2] (data  
594 taken from [3,14,29,36]). Note, all expression patterns are symmetrical, but are shown on one  
595 side only for clarity. cv = cerebral vesicle, fb = forebrain, g = ganglion, hb = hindbrain, mb =  
596 midbrain, n = neck, nc = nerve cord, sc = spinal cord, sv = sensory vesicle.



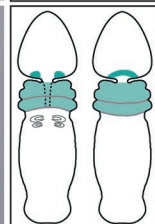
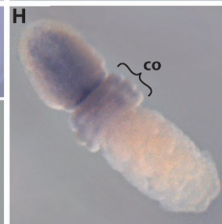
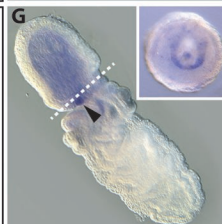
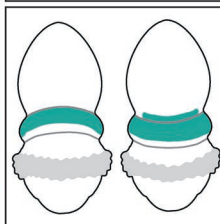
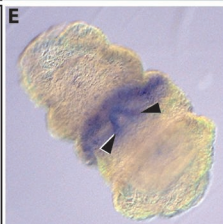
metamorphosing larva

juvenile

six 3/6



otx



engrailed

